

Poly(vinyl benzoate)-b-poly(diallyldimethyl ammonium TFSI) -b-poly(vinyl benzoate) Triblock Copolymer Electrolytes for Sodium Batteries

Pierre L. Stigliano ^{1,2}, Antonela Gallastegui ², Carlos Villacis-Segovia ², Marco Amores ¹, Ajit Kumar ¹, Luke A. O'Dell ¹, Jian Fang ³, David Mecerreyes ^{2,4}, Cristina Pozo-Gonzalo ^{1,5,6} and Maria Forsyth ^{1,4,*}

¹ Institute for Frontier Materials, Deakin University, Geelong, VIC 3216, Australia; pstigliano@deakin.edu.au (P.L.S.); marco.amores@deakin.edu.au (M.A.); ajit.kumar@deakin.edu.au (A.K.); luke.odell@deakin.edu.au (L.A.O.); cristina.pozo@deakin.edu.au (C.P.-G.)

² POLYMAT, University of the Basque Country UPV/EHU, 20018 Donostia-San Sebastian, Spain; antonela.gallastegui@polymat.eu (A.G.); carlos.villacis@polymat.eu (C.V.-S.); david.mecerreyes@ehu.es (D.M.)

³ College of Textile and Clothing Engineering, Soochow University, Suzhou 215123, China; jian.fang@suda.edu.cn

⁴ Ikerbasque, Basque Foundation for Science, María Díaz de Haro 3, 48013 Bilbao, Spain

⁵ ARAID Foundation, Av. de Ranillas 1-D, 50018 Zaragoza, Spain

⁶ Instituto de Carboquímica (ICB-CSIC), Miguel Luesma Castán, 4, 50018 Zaragoza, Spain

* Correspondence: maria.forsyth@deakin.edu.au

Experimental Section

Materials

Sodium bis(fluorosulfonyl)imide (NaFSI) (Solvionic, 99.99% purity) was dried at 50 °C under vacuum overnight and stored in Ar filled glovebox. The polymer electrolyte membranes were prepared as shown in Figure 3, NaFSI and the block copolymer were dissolved in a solvent mixture of tetrahydrofuran (THF) and acetonitrile (ACN). The solution was stirred at RT overnight and then cast on Teflon mold for solvent evaporation. The dry membranes were hot pressed and then dry at RT under vacuum, before being stored in Ar filled glovebox.

Synthesis of PVB-PDADMTFSI-PVB block copolymers

The initial step of the synthesis involved synthesizing the double-functionalized chain transfer agent (CTA), known as X-DiEST-X. Diethyl meso-2,5-dibromoadipate (10 g; 27.7 mmol) was dissolved in 250 mL of 96% ethanol (EtOH) at room temperature in a 500 mL round bottom flask. Subsequently, potassium ethyl xanthogenate was added to the solution and stirred for 90 minutes. The reaction took place at room temperature for 4 hours. Upon completion, the resulting potassium bromide salt was filtered, and ethanol was removed under vacuum. The product was then dissolved in dichloromethane (DCM) and washed three times with distilled water. After evaporating the DCM, the product was dried under vacuum for 24 hours.

The second step involved synthesizing the MacroCTA, denoted as X-PAm-DiEst-PAm-X, to achieve water solubility, a crucial property for the polymerization of PDADMACl. X-DiEst-X (4 g), acrylamide (12.8 g), and radical initiator AIBA (0.098 g) were dissolved in 8 mL of water and 35 mL of ethanol in a 50 mL Schlenk flask. The solution was then deoxygenated using nitrogen for 30 minutes. The reaction proceeded for one hour until a white precipitate formed. The precipitate was subsequently extracted and dried under vacuum at 40 °C overnight. Finally, the product was characterized using ¹H-NMR and MALDI-TOF techniques (Figures S1 and S2).

The polymerization process of the PDADMTFSI block consisted of two stages. The first stage involved synthesizing poly-DADMACl: X-PAm-DiEst-PAm-X (2 g), AIBA (0.088 g), and PDADMACl (15.6 mL, 65 wt% aqueous solution) in a 50 mL Schlenk tube. The mixture was stirred and degassed with nitrogen for 30 minutes. The reactor was then placed in a preheated oil bath set at 60 °C. The final polymer was precipitated using a 1:1 mixture of ethanol and acetone, followed by filtration and vacuum drying at 40 °C. The product was analyzed using ¹H-NMR in D₂O (Figure S3).

Once the PDADMACl polymer was obtained, an anion exchange was conducted to yield PDADMTFSI. PDADMACl was dissolved in distilled water and slowly added to a solution containing LiTFSI and distilled water under magnetic stirring. The resulting precipitate was then separated from the solvent, dried under vacuum at 40 °C overnight, and subsequently characterized using GPC-SEC (Figure S4). Two chain lengths of PDADMTFSI were investigated in this work: 33K and 17.5K, as shown in Table 1

To obtain the final product, PVB-b-PDADMTFSI-b-PVB triblock copolymers, PDADMTFSI and vinyl benzoate were dissolved in dimethylformamide (DMF) with AIBN as the initiator. The solution was deoxygenated with nitrogen for 30 minutes and then immersed in a preheated oil bath at 65 °C.

After 24 hours of reaction, the final polymer was precipitated in cold ethanol, dried under vacuum at 40 °C for 24 hours, and the structure was characterized through ¹H-NMR (Figure S5-8).

MALDI-TOF

For MALDI-TOF measurements a Bruker Autoflex Speed system (Bruker, Germany) integrated with a Smartbeam-II laser (Nd:YAG, 355nm, 2 kHz) was used, with laser power adjusted during the measurements. The spectrum was acquired in linear mode with an average of 5000 shots. Samples were mixed in MeOH at a concentration of 10 mg/mL. The matrix used was 2,5-DHB, dissolved in MeOH at a concentration of 20 mg/mL. NaTFA was the cation donor (10 mg/mL dissolved in MeOH). A matrix/polymer/salt solution with 10:5:1 ratio was used and 0.5 µL were hand-spotted on the ground steel target plate.

Gas Permeation Chromatography (GPC)

For GPC a 1200 Infinity gel permeation chromatograph (GPC, Agilent Technologies) integrated with IR detector, a PLgel 5 mm MIXED-D column and a PLgel guard column (Agilent Technologies) was used. As eluent a 0,1 M LiTFSI/DMF solution was used and flow rate was set at 1.0 mL min⁻¹ at 50 °C. PMMA standards (Agilent Technologies, Mp = 0.55 - 1568 x103) were used to perform calibration.

Differential Scanning Calorimetry (DSC)

Thermal properties of the neat block copolymers and polymer electrolyte membranes were measured by Netzsch DSC (214Polyma). All samples were characterized in the range of -100 and 150 °C, with a heating rate of 40K/min. The second heating is reported.

Fourier Transform Infrared Spectroscopy (FTIR)

The samples were measured by a Perkin Elmer instrument using a single diamond attenuated reflection unit. The spectra were measured in the region from 4000 to 650 cm⁻¹

Transmission Electron Microscopy (TEM)

Block copolymer films were placed into freshly prepared Procure 812 resin (ProSciTech Kirwan, QLD, C045) for 2 hours under vacuum infiltration at RT. The samples were then removed and put in resin mold (Procure 812 resin) before curing for 3 days at 58°C. The resin block was sectioned using a Leica UC7 ultramicrotome to obtain silver interference (~50nm) sections and collected onto EMSFCFTH 400 mesh copper grids (ProSciTech Kirwan, QLD). Samples were imaged using a Tecnai 12 Transmission Electron Microscope (FEI, Eindhoven, The Netherlands), operating voltage of 120 kV. At all times low dose procedures were followed, using an electron dose of less than 5 electrons/Å² for all imaging. Images were recorded using a FEI Eagle 4k x 4k CCD camera at a range of magnifications using AnalySIS v3.2 camera control software (Olympus).

Solid State Magic Angle Spin Nuclear Magnetic Resonance Spectroscopy (MAS-NMR)

For NMR spectroscopy, a Bruker Avance III 500 MHz ultra shield wide bore spectrometer was used. Zirconia MAS NMR rotors (diameter: 1.3 mm) were filled with samples inside Ar filled glovebox. Spectra were analysed using TopSpin software. Full-width half-maximum (fwhm) values were calculated by fitting the peaks with Gaussian/Lorentzian function.

Ionic Conductivity

Ionic conductivity was measured using MTZ-35 in the frequency range of 1 Hz to 10 MHz (amplitude of 0.01 V) in the temperature range of 30 and 90 °C. The polymer electrolyte membranes were cut into 12 mm diameter round discs and sandwiched between two stainless steel electrodes inside of a coin cell. The coin cell was then put in a custom-built barrel cell. All the spectra were fitted by MT-lab software.

Electrochemical Characterization

T_{Na^+} at 70 °C was measured with the Bruce–Vincent method, the equation used for calculation is:

$$T_{Na^+} = \frac{I_s(\Delta V - I_0 R_{io})}{I_0(\Delta V - I_s R_{is})}$$

Where ΔV = applied constant potential, I_0 and I_s = initial and steady-state currents, respectively, and R_{io} and R_{is} = initial and steady state interfacial resistance, respectively.

Na|Na symmetric cell cycling was performed using a coin cell with the electrolyte membrane (thickness 300 μm , diameter 14 mm) sandwiched between 2 Na metal discs (diameter 10 mm). Cells were assembled inside an Ar filled glovebox. Na-metal stripping and plating were studied at different currents using a Biologic VMP3 potentiostat, data were processed with EC-Lab software.

A homemade 2-electrode Swagelok-type cell was employed for Sodium-Air Battery (SAB) testing. The cell parts were dried at 60 °C overnight and then transferred to an Ar filled glovebox for assembling. The SAB cell was composed of a sodium metal disk (diameter = 12 mm, Sigma Aldrich), the polymer electrolyte membrane (diameter = 12.7 mm) and multi-doped carbon nanofibers air cathode (reported in literature). The surface of the air cathode was wetted with 50 μL of liquid electrolyte (NaTFSI:diglyme: $\text{C}_4\text{mpyrTFSI}$ in mol ratio 1:4:1) to improve contact between air cathode and polymer electrolyte membrane. Once assembled, the cells were taken outside of the Ar filled glovebox and pressurized under pure oxygen (99.99% purity). The cells were left to rest for 8 h at open circuit voltage and 50 °C. Subsequently, a current density of $-75 \mu\text{A cm}^{-2}$ was applied, with a cut-off potential of 1.6 V.

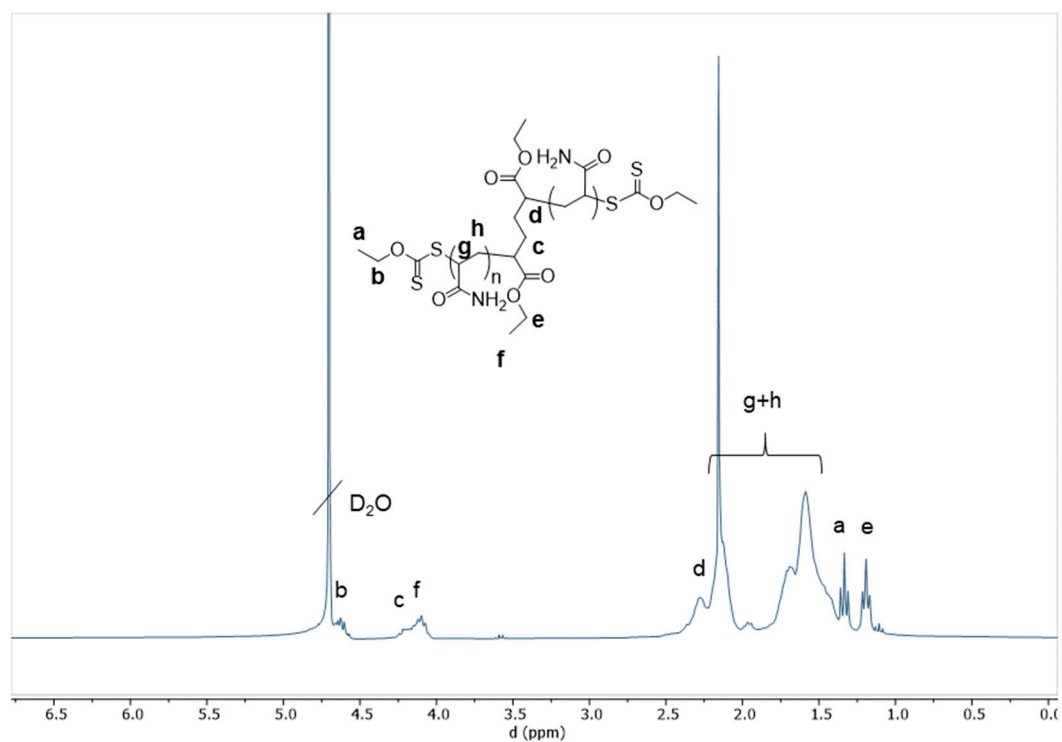


Figure S1 $^1\text{H-NMR}$ (300 MHz) di funcional CTA X-PAM-DiEst-PAM-X in D_2O (the * indicates the ethanol remaining from the purification)

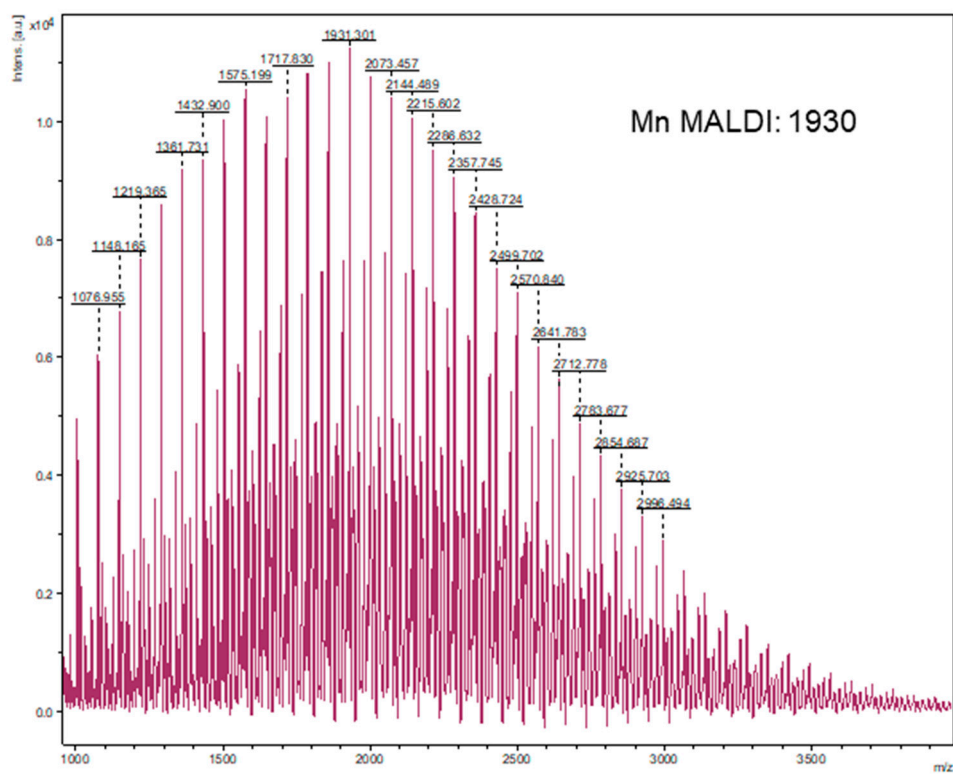


Figure S2 MALDI-TOF analysis of X-Pam-DiEst-Pam-X (X-AdA-X)

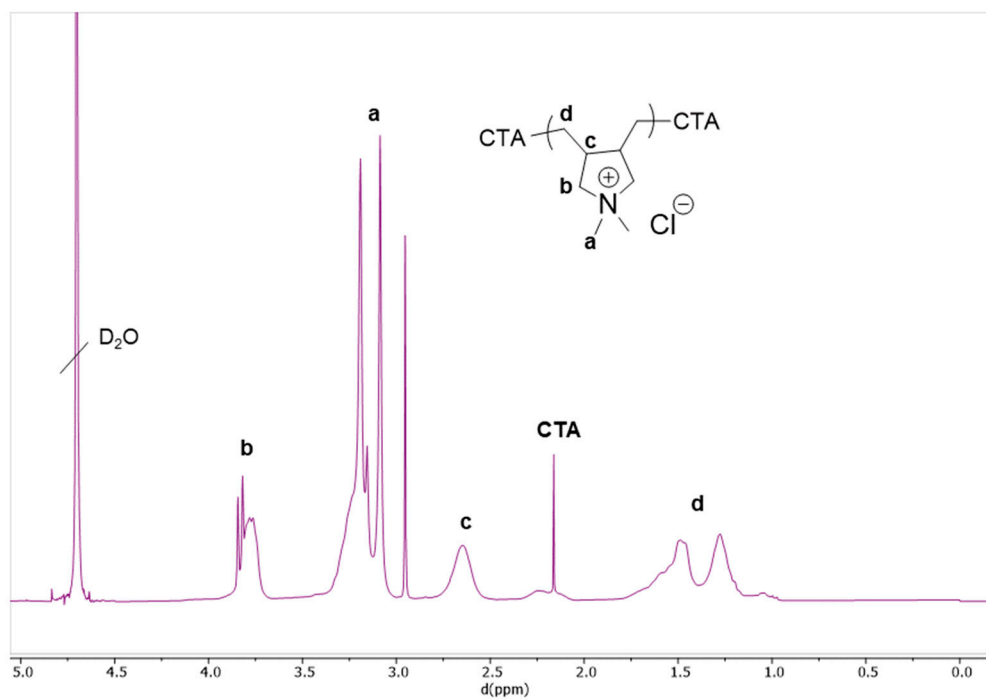


Figure S3 ^1H -NMR (300 MHz) of MacroCTA in D_2O

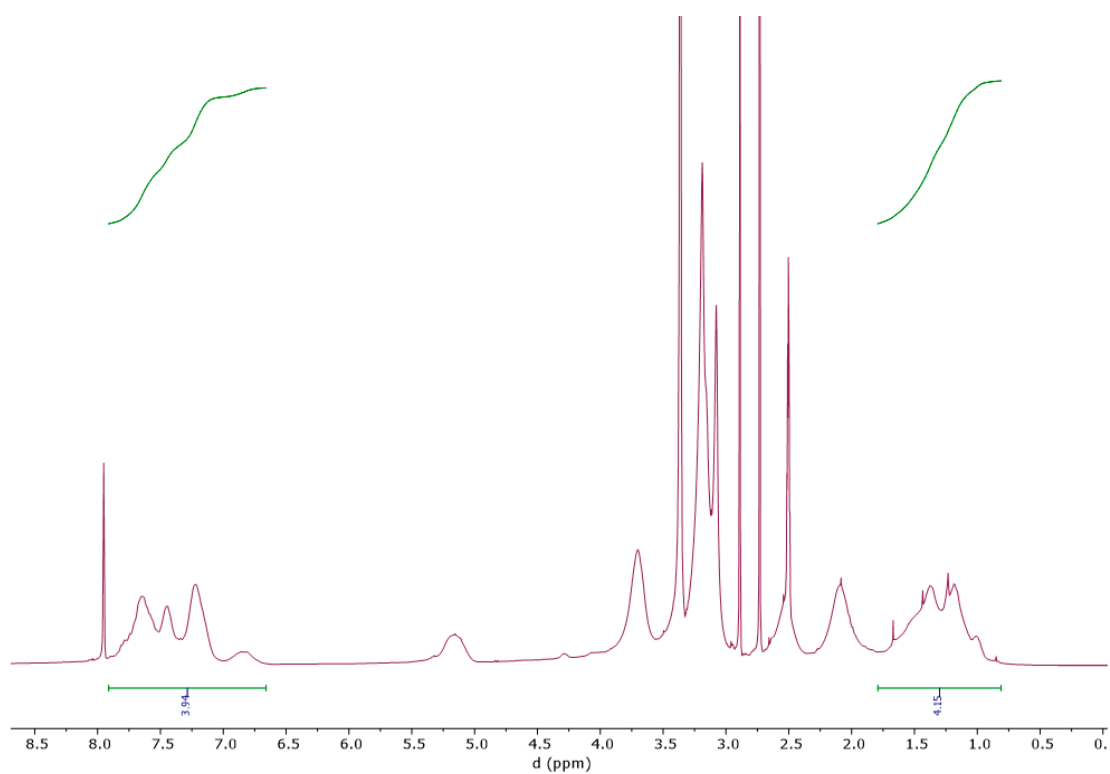


Figure S4 ^1H -NMR of $\text{PVB}_{11.5\text{K}}-b\text{-PDADMATFSI}_{33\text{K}}-b\text{-PVB}_{11.5\text{K}}$

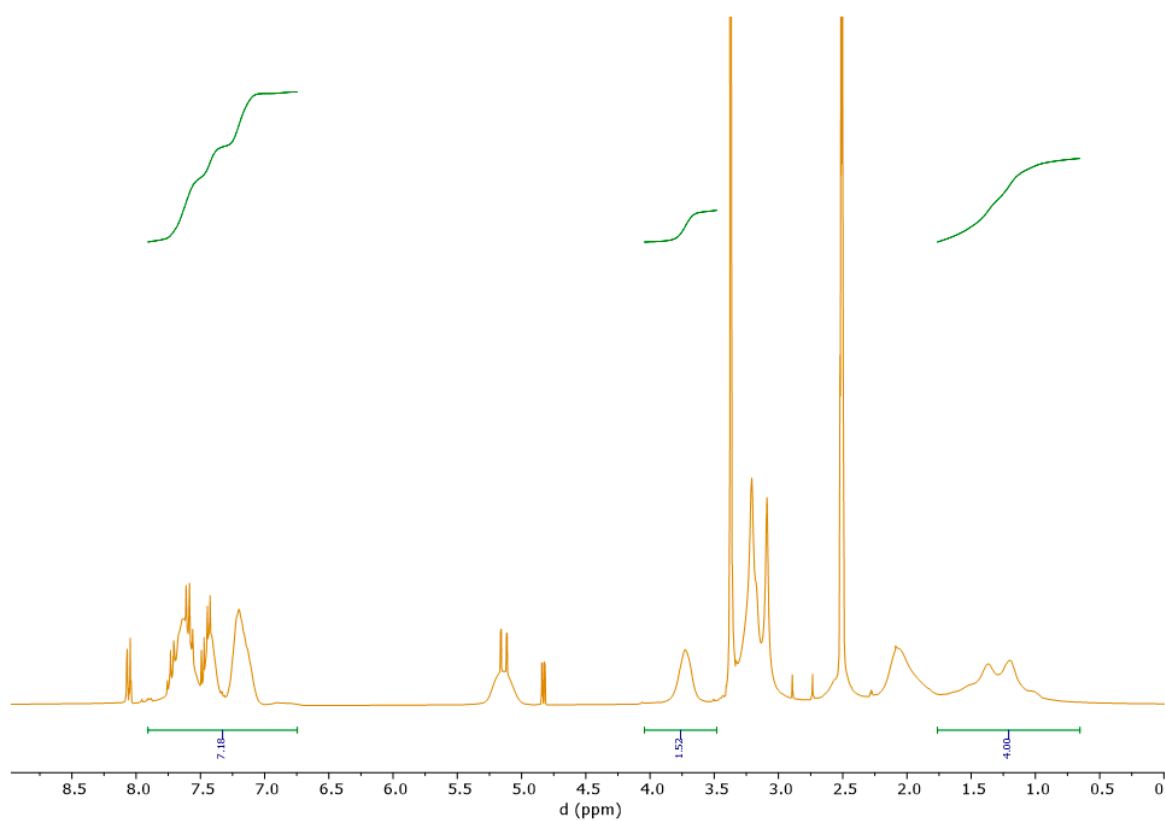


Figure S5 ^1H -NMR of $\text{PVB}_{11.5\text{K}}\text{-}b\text{-PDADMATFSI}_{17.5\text{K}}\text{-}b\text{-PVB}_{11.5\text{K}}$

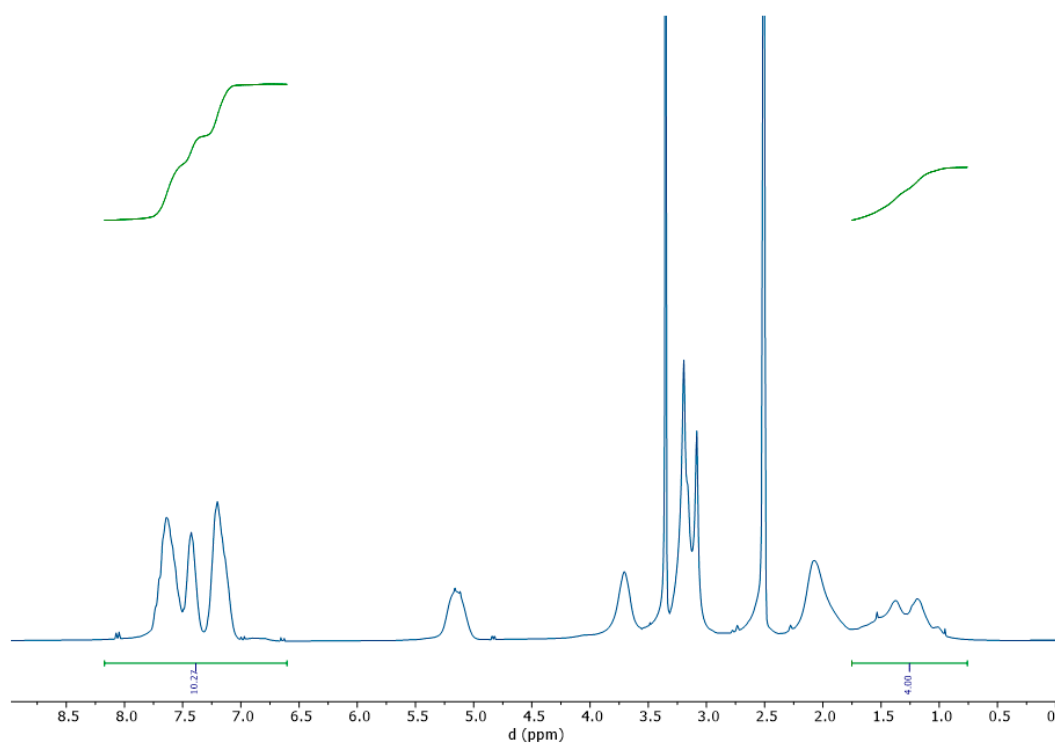


Figure S6 ^1H -NMR of $\text{PVB}_{22.5\text{K}}\text{-}b\text{-PDADMATFSI}_{33\text{K}}\text{-}b\text{-PVB}_{22.5\text{K}}$

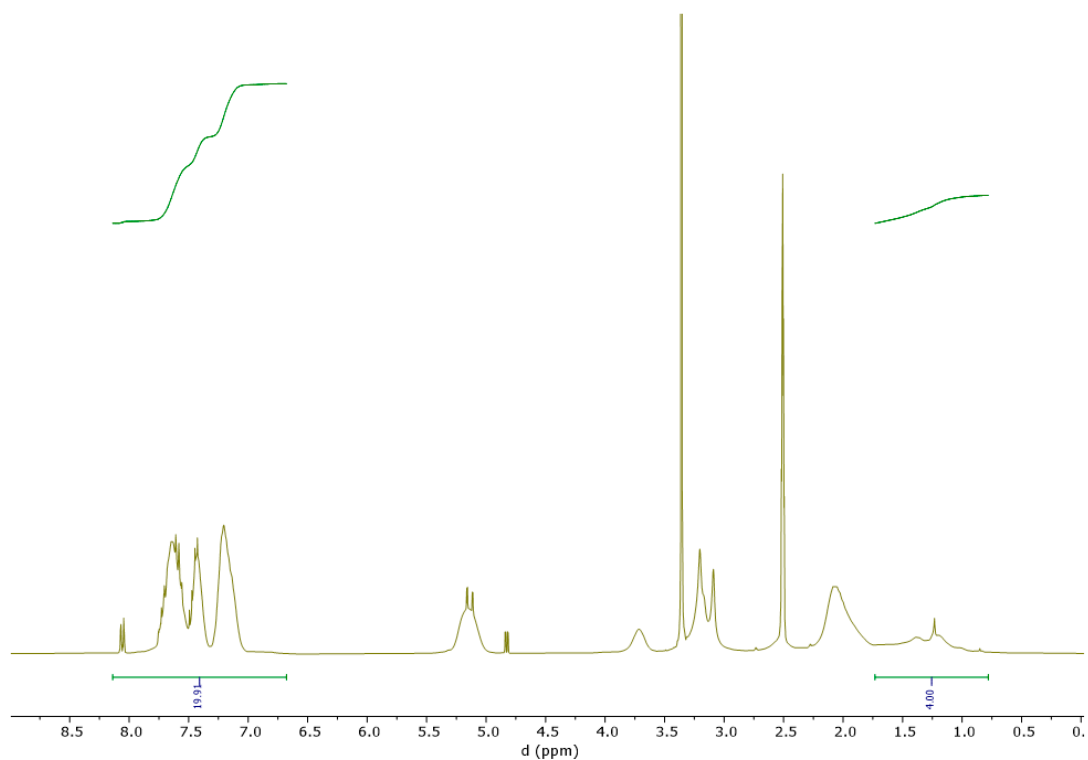


Figure S7 ^1H -NMR of $\text{PVB}_{22.5\text{K}} - b - \text{PDADMATFSI}_{17.5\text{K}} - b - \text{PVB}_{22.5\text{K}}$

Table S1 FTIR absorption band positions and assignment for neat PVB-PDADMAT-PVB BCPs

IR vibration frequency (cm ⁻¹)		Bond Assignment
Component		
[PDADMA][TFSI]	PVB	
	1711	C=O
1640		βC–N of P(DADMA) ⁺
	1584	C=C benzoate ring
1476		δCH ₃ of P(DADMA) ⁺
	1451	C-C (in ring)
1345		ν _{as} SO ₂ (IP)
1332		ν _{as} SO ₂ (OP)
	1269	C-O
1175		ν _{as} CF ₃ of TFSI ⁻
1132		ν _s SO ₂ of TFSI ⁻
1053		δCF ₃ of TFSI ⁻
789		S–N stretch/δCF ₃ of TFSI ⁻

741		$v_s(\text{S-N-S})$
	707	C-H out-of-plane
656		$\delta(\text{SNS})$

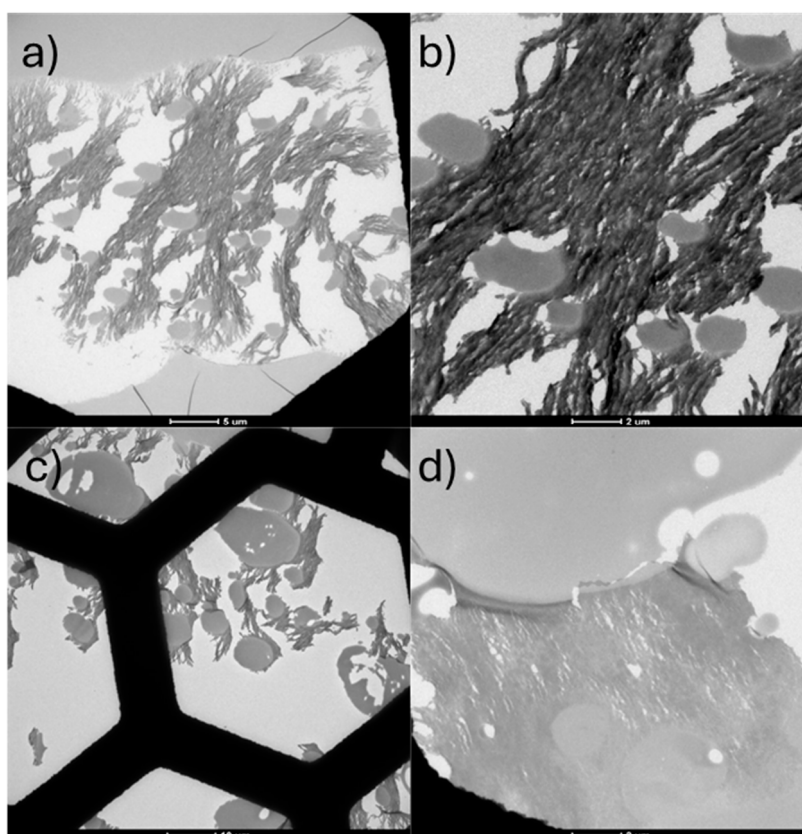


Figure S8 TEM images of BCP BCP-1233 (a,b) and BCP-2218 (c,d)

In Figure S9, Transmission Electron Microscopy (TEM) images provide detailed insights into the microstructure of neat BCP-1233 and BCP-2218. Examining BCP-1233, two distinct structures are discernible: light grey aggregates ranging in size from 1 to 3 μm in diameter and elongated wormlike micelles approximately 500 nm in width. Notably, the elongated wormlike micelles exhibit signs of separation under certain shear stress conditions. Phase separation between the PVB and PDADMATFSI blocks becomes apparent, with the inference that the light grey aggregates predominantly consist of PVB, while the elongated wormlike micelles are attributed to PDADMATFSI. Turning attention to BCP-2218, similar dual structures are observed, but with distinct features. Here, the aggregates display a larger size, exceeding 10 μm in diameter, while the elongated wormlike micelles exhibit a reduced width. Macroscopic phase separation is once again evident, aligning with the inferred proposition that the aggregates are formed by PVB

and the micelles by PDADMATFSI. The TEM imaging further illustrates how both samples exhibit the presence of pores across the different phases.

Table S2 Sample name and characteristics of the membrane with 2:1 Na:PDADMATFSI mol ratio for all four compositions of neat polymer

Sample Name	Total Mw (Neat polymer)	mol/g of neat polymer	mol/g of PDADMATFSI	mol/g of PVB	Na:Polymer mol ratio	NaFSI wt%
BCP-12 33 -Na	56000	8.92E-06	1.2E-03	0.0007	0.70	35.4
BCP-12 18 -Na	40500	1.23E-05	1.7E-03	0.0005	0.44	28.7
BCP-23 33 -Na	78000	6.41E-06	1.7E-03	0.0005	0.43	28.3
BCP-23 18 -Na	62500	8.00E-06	2.1E-03	0.0003	0.25	20.7

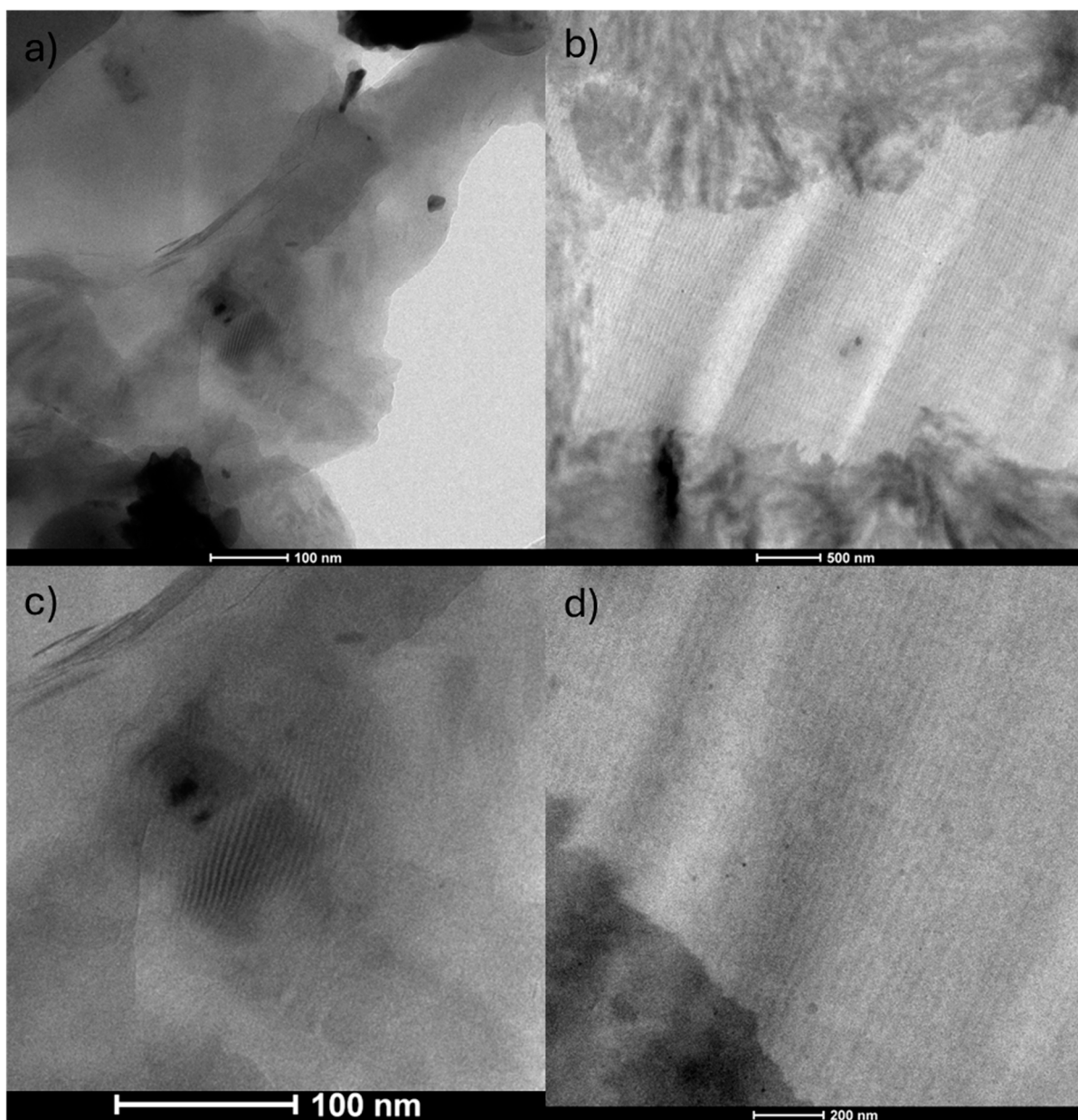


Figure S9 TEM images of BCP BCP-1233-Na (a,c) and BCP-2218-Na (b,d)

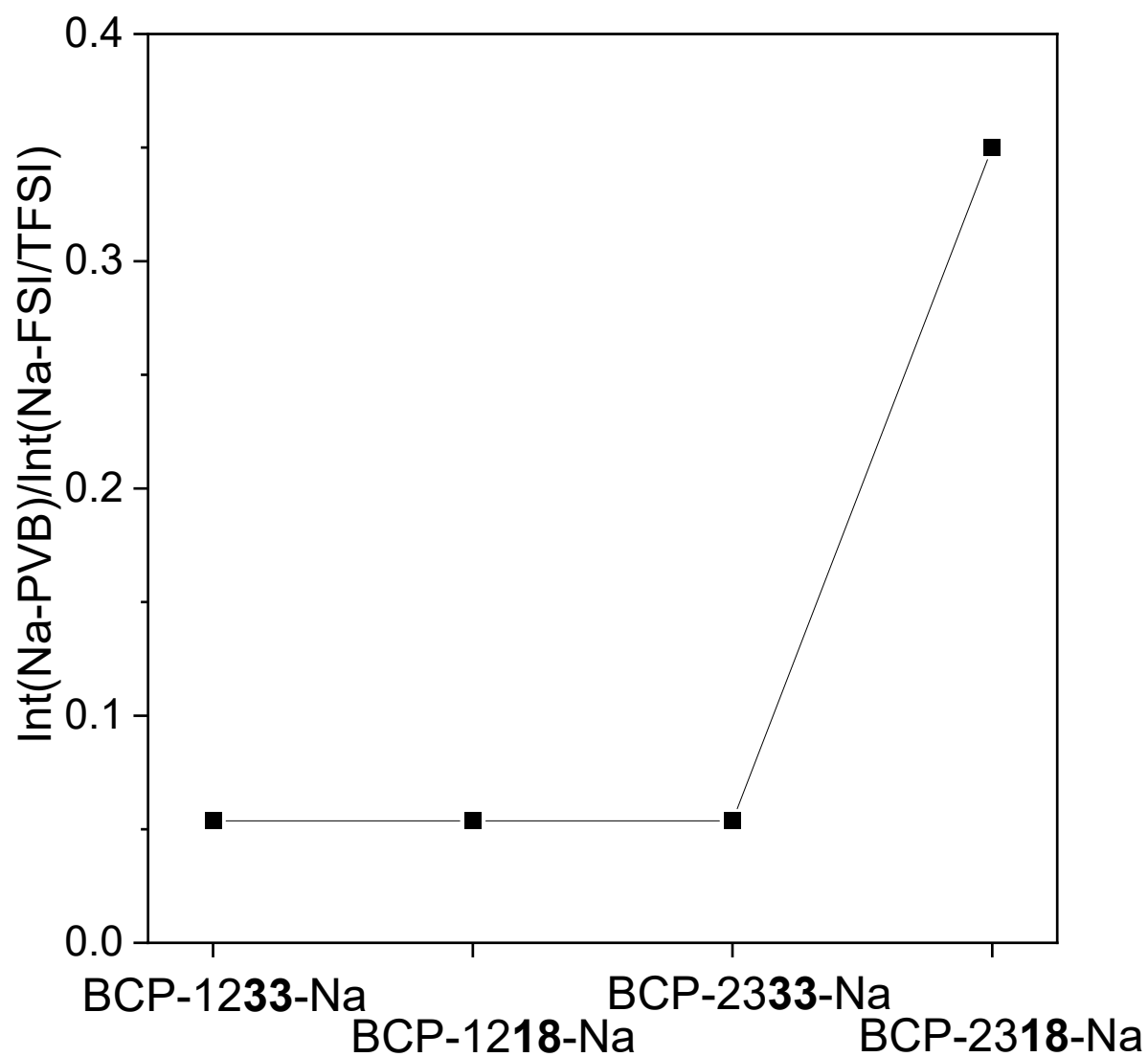


Figure 10 Ratio between integrals of the two coordination peaks observed in ^{23}Na NMR

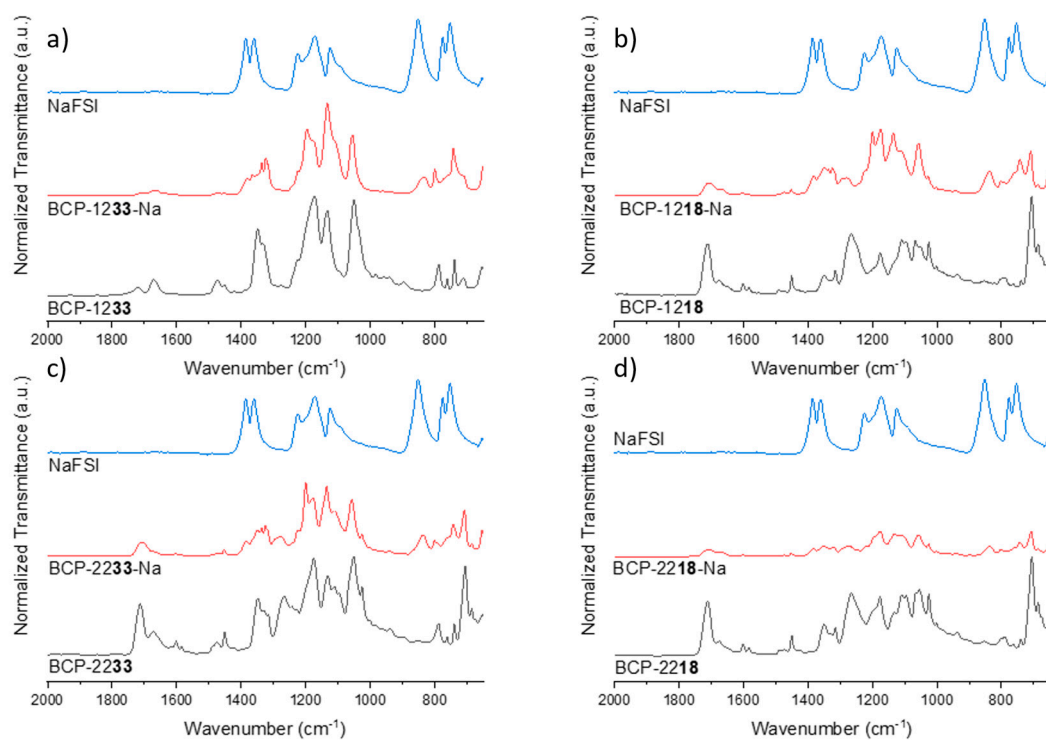


Figure S11 FTIR spectra of neat BCP and BCP-NaFSI mixtures with a 2:1 Na:PDADMA mol ratio

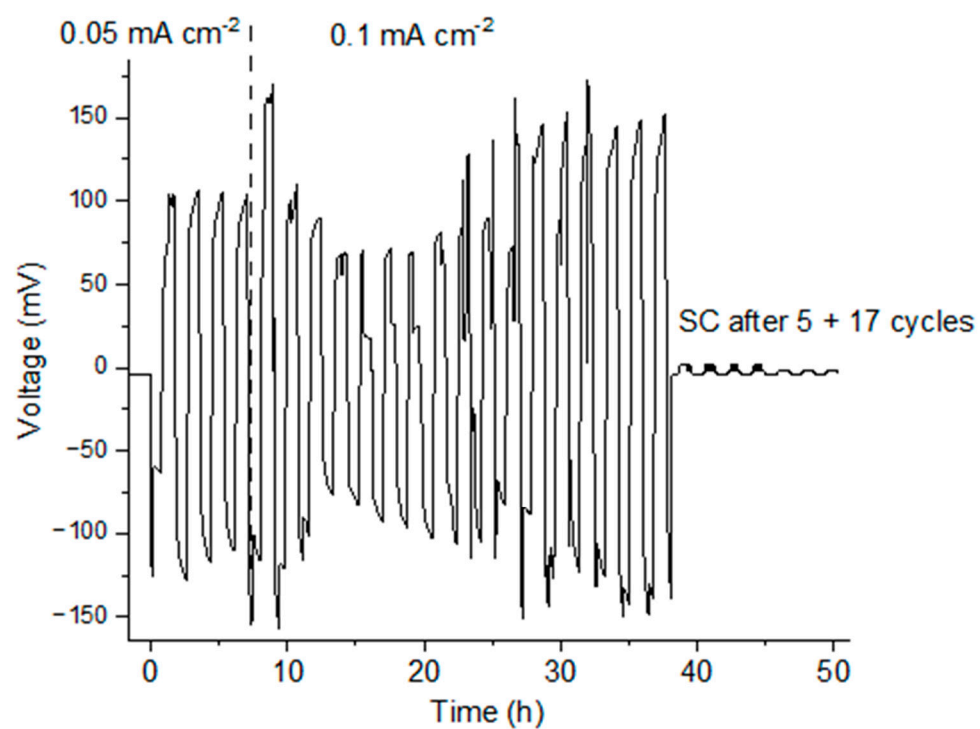


Figure S12 Galvanostatic cycling of sodium symmetrical cells using BCP-1233-Na at 70 °C



Figure S13 Photo of the membrane after galvanostatic cycling in Na|Na cells showing the formation of large dendrites

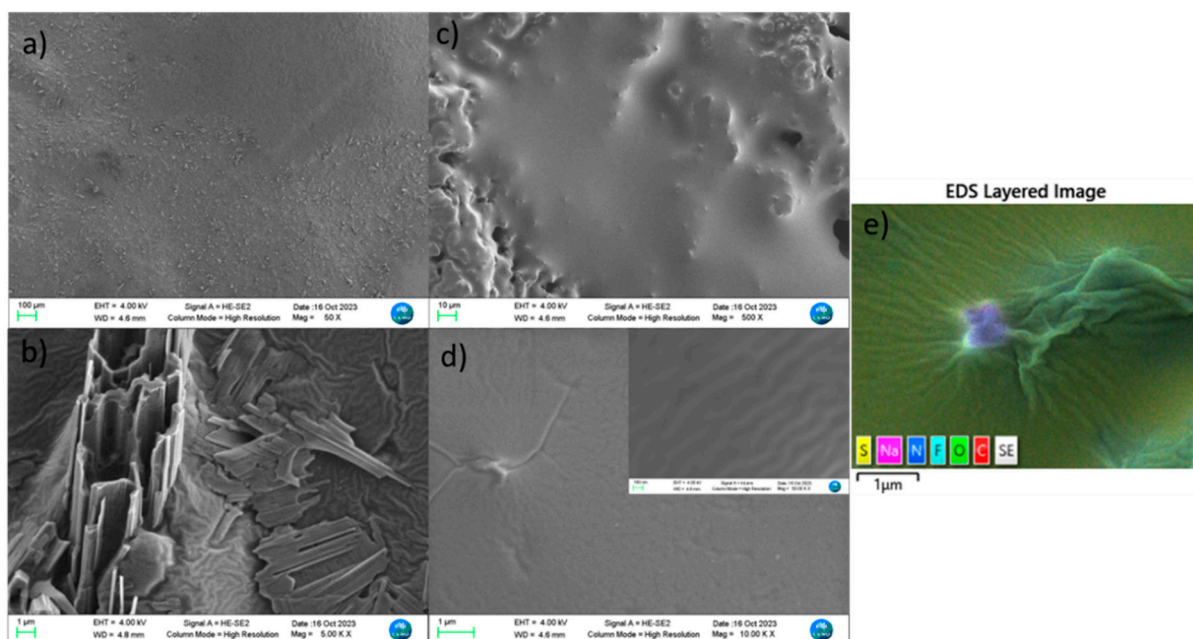


Figure S14 SEM images of the surface of BCP-1233-Na (a,b) and BCP-2218-Na (c,d); e) EDS layered image zoomed on one of the structures found on the surface of BCP-2218-Na as seen in figure 7d

Scanning electron microscopy (SEM) and Energy-dispersive X-ray (EDX) spectroscopy were used to investigate the surface topology and composition of the polymer membranes.

In figure 7 are shown the SEM images of the surface of BCP-1233-Na and BCP-2218-Na. From SEM imaging of the surface of the polymer electrolyte membranes we can see how the phase separation observed by TEM in the neat polymers (Figure 2) is still present, although it is not as evident as observed in the neat polymers.

The SEM analysis of BCP-1233(2 (Figure 7a and b) shows the presence of structures originating on and piercing through the surface. Upon closer inspection (Figure 7b), these structures reveal a hollow nature and are encompassed by organized systems, exhibiting a conformation similar to the lamellae observed in the TEM images of the neat polymer (Figure 2c,d). This observation suggests a potential correlation between the structures in question and the lamellae formations in the neat polymer, although with a different spatial arrangement because of the casting method used.

By comparing the width of the lamellar structures (PDADMTFSI) in the neat polymer and in the electrolyte membranes, it results that the introduction of NaFSI results in a discernible reduction in width, indicative of a structural modification within the polymer during the casting of the electrolyte membranes.

For BCP-2218-Na, SEM analysis (Figure 7c,d) accentuates the phase separation between the two blocks, revealing a surface with distinct rough and smooth regions. The smooth surface exhibits agglomerated structures, primarily composed of Na and F, as verified by energy-dispersive X-ray spectroscopy (EDS) analysis (Figure 7e). Surrounding the agglomerated structures is an organized system exhibiting a lamellar structure, prominently illustrated in the inset of Figure 7d and the layered EDS image. Once again, the lamellar structure identified on the surface of the polymer electrolyte membrane is found to be narrower than the lamellae observed by TEM in the neat polymer (Figure 2e,f).

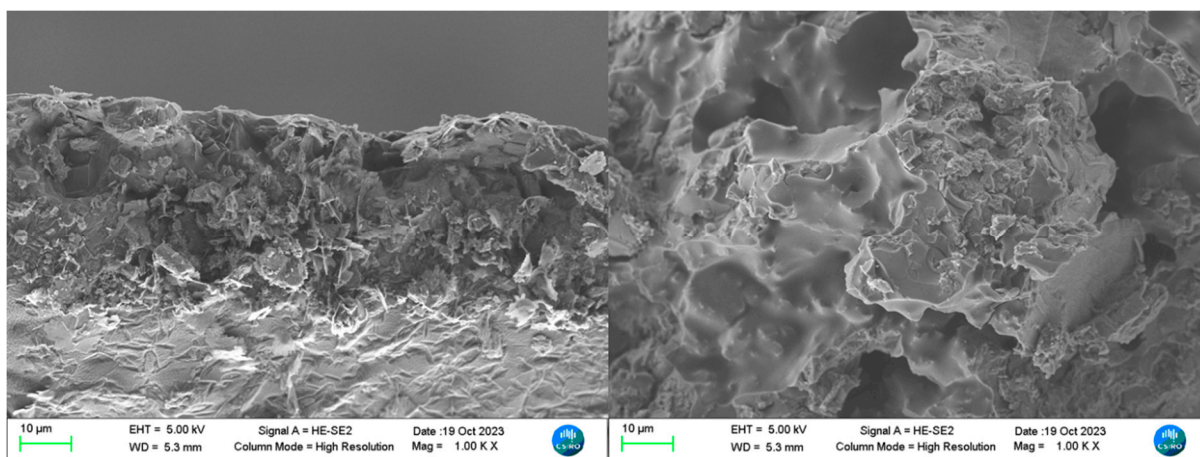


Figure S15 SEM images of the cross-section of BCP-1233-Na

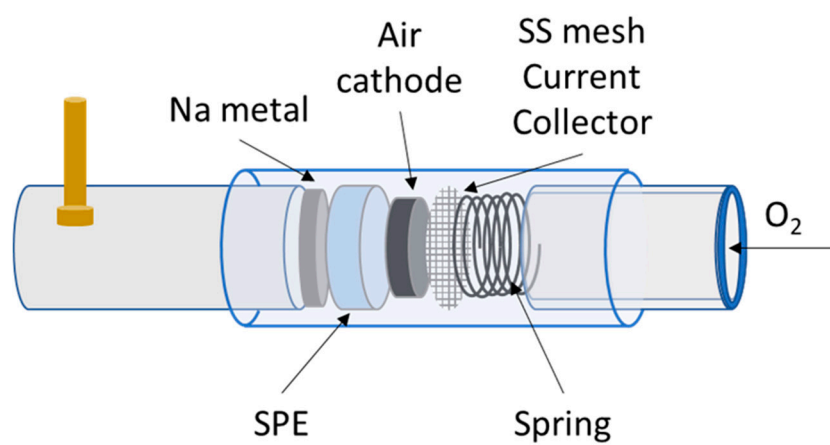


Figure S16 Cell configuration of the home modified Swagelok-type Na-O₂ cell used